

This is the **accepted version** of the journal article:

Crowther, T. W.; Todd-Brown, K. E. O.; Rowe, C. W.; [et al.]. «Quantifying global soil carbon losses in response to warming». Nature, Vol. 540 (November 2016), p. 104-108. DOI 10.1038/nature20150

This version is available at <https://ddd.uab.cat/record/299923>

under the terms of the  ^{IN} COPYRIGHT license

1 QUANTIFYING GLOBAL SOIL C LOSSES IN RESPONSE TO WARMING

2
3 Crowther, T.W.^{1,2}, Todd-Brown, K.E.O.³, Rowe, C.W.², Wieder, W.R.^{4,5}, Carey, J.C.⁶,
4 Machmuller, M.B.⁷, Snoek, L.B.^{1,8}, Fang, S.^{9,10}, Zhou, G.⁹, Allison, S.D.^{11,12}, Blair,
5 J.M.¹³, Bridgham, S.D.¹⁴, Burton, A.J.¹⁵, Carrillo, Y.¹⁵, Reich, P.B.^{16,17}, Clark, J.S.¹⁸,
6 Classen, A.T.^{19,20}, Dijkstra, F.A.²¹, Elberling, B.²², Emmett, B.²³, Estiarte, M.^{24,25}, Frey,
7 S.D.²⁶, Guo, J.²⁷, Harte, J.²⁸, Jiang, L.²⁹, Johnson, B.R.¹⁴, Kröel-Dulay, G.³⁰, Larsen,
8 K.S.³¹, Laudon, H.³², Lavallee, J.M.^{7,33}, Luo, Y.²⁹, Lupascu, M.³⁴, Ma, L.N.³⁵, Marhan,
9 S.³⁶, Michelsen, A.³⁷, Mohan, J.^{38,39}, Niu, S.⁴⁰, Pendall, E.¹⁶, Peñuelas, J.^{24,25}, Pfeifer-
10 Meister, L.¹⁴, Poll, C.³⁶, Reinsch, S.²³, Reynolds, L.L.¹⁴, Schmidt, I.K.³⁰, Sistla, S.⁴¹,
11 Sokol, N.W.³, Templer, P.H.⁴², Treseder, K.K.¹², Welker, J.M.⁴³, & Bradford, M.A.^{1,2}

- 12
- 13 1. Netherlands Institute of Ecology, Droevendaalsesteeg 10, 6708 PB Wageningen,
- 14 The Netherlands
- 15 2. Yale School of Forestry & Environmental Studies, Yale University, 370 Prospect
- 16 St., New Haven, CT 06511, USA
- 17 3. Pacific Northwest National Laboratory, Richland, WA, USA
- 18 4. Climate & Global Dynamics Laboratory, National Center for Atmospheric
- 19 Research, Boulder, CO 80307, USA
- 20 5. Institute for Arctic & Alpine Research, University of Colorado, Boulder, CO
- 21 80303, USA
- 22 6. Marine Biological Laboratory, 7 MBL St., Woods Hole, MA 02543, USA
- 23 7. Natural Resource Ecology Laboratory, 1499 Campus Delivery, Colorado State
- 24 University, Fort Collins, CO, 80523-1499, USA
- 25 8. Laboratory of Nematology, Wageningen University, Droevendaalsesteeg 1, 6708
- 26 PB Wageningen, The Netherlands
- 27 9. Chinese Academy of Meteorological Sciences, No.46 Zhongguancun South
- 28 Street, Beijing 100081, China
- 29 10. Collaborative Innovation Center on Forecast Meteorological Disaster
- 30 Warning & Assessment, Nanjing University of Information Science &
- 31 Technology, Nanjing 210044, China

- 32 11. Department of Earth System Science, University of California Irvine,
33 Irvine, CA 92697, USA
- 34 12. Department of Ecology & Evolutionary Biology, University of California
35 Irvine, CA 92697, USA
- 36 13. Division of Biology, Kansas State University, Manhattan, KS 66506, USA
- 37 14. Institute of Ecology & Evolution, University of Oregon, Eugene, OR
38 97403, USA
- 39 15. School of Forest Resources & Environmental Science, Michigan
40 Technological University, Houghton, MI 49931, USA
- 41 16. Hawkesbury Institute for the Environment, Western Sydney University, Penrith,
42 2570 NSW, Australia
- 43 17. Department of Forest Resources, University of Minnesota, St. Paul, MN 55108,
44 USA
- 45 18. Nicholas School of the Environment, Duke University, Durham, NC 27708, USA
- 46 19. Department of Ecology & Evolutionary Biology, University of Tennessee, 569
47 Dabney Hall, 1416 Circle Dr., Knoxville, TN 37996, USA
- 48 20. The Natural History Museum of Denmark, University of Copenhagen,
49 Universitetsparken, 15, 2100, København Ø, Denmark
- 50 21. Centre for Carbon, Water & Food, The University of Sydney, Camden, 2570
51 NSW, Australia
- 52 22. Center for Permafrost (CENPERM), Department of Geosciences and Natural
53 Resource Management, University of Copenhagen, Øster Voldgade 10, 1350
54 Copenhagen K., Denmark
- 55 23. Environment Centre Wales, Deiniol Rd, Bangor. LL57 2UW, UK
- 56 24. CSIC, Global Ecology Unit CREAM-CSIC-UAB, Cerdanyola del Vallès, 08193
57 Catalonia, Spain
- 58 25. CREAM, Cerdanyola del Vallès, 08193 Catalonia, Spain.
- 59 26. Department of Natural Resources & the Environment, University of New
60 Hampshire, Durham, NH 03824, USA
- 61 27. Key Laboratory of Vegetation Ecology, Ministry of Education, Northeast Normal
62 University, Changchun 130024, Jilin Province, China

- 63 28. Energy & Resources Group, University of California at Berkeley, Berkeley, CA
64 94720, USA
- 65 29. Department of Microbiology & Plant Biology, University of Oklahoma, Norman,
66 OK 73019, USA
- 67 30. Institute of Ecology & Botany, MTA Centre for Ecological Research, 2-4.
68 Alkotmany U., Vacratot, 2163-Hungary
- 69 31. Department of Geosciences & Natural Resource Management, University of
70 Copenhagen, Rolighedsvej 23, 1958 Frederiksberg C, Denmark
- 71 32. Department of Forest Ecology & Management, Swedish University of
72 Agricultural Sciences, 90183 Umeå, Sweden
- 73 33. Faculty of Life Sciences, University of Manchester, Dover Street, Manchester
74 M13 9PT, UK
- 75 34. Department of Geography, National University of Singapore, 10 Kent Ridge
76 Crescent, 119260, Singapore
- 77 35. State Key Laboratory of Vegetation & Environmental Change, Institute of
78 Botany, Chinese Academy of Sciences, Beijing, 100093, China
- 79 36. Institute of Soil Science & Land Evaluation, University of Hohenheim, 70593
80 Stuttgart, Germany
- 81 37. Department of Biology, University of Copenhagen, Universitetsparken 15, DK-
82 2100 Copenhagen, Denmark
- 83 38. Odum School of Ecology, University of Georgia, Athens, GA 30601, USA
- 84 39. Center for Permafrost, University of Copenhagen, Øster Voldgade 10, DK-1350
85 Copenhagen K, Denmark
- 86 40. Key Laboratory of Ecosystem Network Observation & Modeling, Institute of
87 Geographic Sciences and Natural Resources Research, Chinese Academy of
88 Sciences, Beijing, 100101, China
- 89 41. School of Natural Science, Hampshire College, 893 West St., Amherst MA
90 01002, USA
- 91 42. Department of Biology, Boston University, Boston, MA 02215, USA
- 92 43. Department of Biological Sciences, University of Alaska, Anchorage, Anchorage,
93 AK 99508, USA

94 **Generating meaningful greenhouse gas (GHG) emission targets requires an**
95 **understanding of Earth system dynamics and projections about how they will**
96 **respond to global change¹⁻³. If anthropogenic warming stimulates the loss of carbon**
97 **from the Earth's surface into the atmosphere, it could drive additional planetary**
98 **warming. Despite growing evidence that warming enhances soil carbon fluxes to and**
99 **from the soil^{8,12}, the net global balance between these responses remains uncertain¹.**
100 **Here we present a comprehensive analysis of warming-induced changes in soil**
101 **carbon stocks by assembling data from 49 field experiments located across North**
102 **America, Europe and Asia. We find that the effects of warming are contingent upon**
103 **the size of the initial soil carbon stock, with considerable carbon losses occurring in**
104 **high-latitude areas. By extrapolating this empirical relationship to the global scale,**
105 **we provide estimates of global soil carbon sensitivity that may help to constrain**
106 **Earth System Model projections. Our empirical relationship suggests that global**
107 **soil carbon stocks in the upper soil horizons will fall by 30 (\pm 30) to 203 (\pm 161) Pg C**
108 **for 1 degree of continuous warming, depending upon the potential acclimatization**
109 **rate of soil organic matter decomposition. An assumption of annual acclimation**
110 **yields a conservative estimate that soil C stocks will fall by 55 (\pm 50) Pg C from the**
111 **upper soil horizons by 2050, a value that is 12-17% of anthropogenic emissions over**
112 **this period. Despite the uncertainty in these estimates, the direction of the global soil**
113 **carbon response is consistent across all acclimatization scenarios. Our analysis**
114 **provides strong empirical support for the assumption that rising temperatures will**
115 **stimulate the net loss of soil carbon to the atmosphere, driving a positive land**
116 **carbon-climate feedback that could accelerate climatic change.**

117

118 The majority of the Earth's terrestrial C is stored in the soil and changes in the size of this
119 C stock represent a prominent control on atmospheric C concentrations⁶⁻⁸. If
120 anthropogenic warming stimulates the loss of even a small proportion of soil C, it could
121 drive substantive additional planetary warming^{7,9}. Yet, despite considerable scientific
122 attention in recent decades, there remains no consensus on the direction or magnitude of
123 warming-induced changes in soil C^{3,10}. Although there is growing confidence that
124 warming generally enhances fluxes to and from the soil^{8,12}, the net global balance

125 between these responses remains uncertain and direct estimates of soil C stocks are
126 limited to single-site experiments that generally reveal no detectable effects^{1,11-13}.
127
128 Given the paucity of direct measurements of soil C stock responses to warming, Earth
129 System Models (ESMs) must rely heavily on short-term temperature responses of soil
130 respiration (Q_{10}) to infer long-term changes in global C stocks. Without empirical
131 observations that capture longer-term C dynamics, we are limited in our ability to
132 evaluate model performance, or constrain the uncertainty in model projections¹⁴. As such,
133 the land C-climate feedback remains one of the largest sources of uncertainty in current
134 ESMs¹⁻³, restricting our capacity to develop C emissions targets that are compatible with
135 specific climate change scenarios. Direct field measurements of warming-induced
136 changes in soil C stocks are urgently needed to increase confidence in future climate
137 projections¹⁴.

138
139 We take advantage of the growing number of climate change experiments around the
140 world to compile the first global database of soil C stock responses to warming. Soil
141 samples were collected from replicate plots in 49 climate change experiments conducted
142 across six biomes, ranging from arctic permafrost to dry Mediterranean forests (Extended
143 data Figure 1). We compared soil C stocks across ‘warmed’ (treatment) and ‘ambient’
144 (control) plots to explore the effects of temperature across sites. The measured
145 differences in soil C stocks represent the net result of long-term changes in soil C inputs
146 (plant production) and outputs (respiration) in response to warming. By linking these soil
147 C responses to climatic and soil characteristics we are able to generate a spatial
148 understanding of the temperature-sensitivity of soil C stocks at a global scale. To
149 standardise collection protocols and account for the considerable variability in soil
150 horizon depths, we focus on C stocks in the top 10 cm of soil. At a global scale, this
151 upper soil horizon contains the greatest proportion of biologically active soil C by depth⁶.

152
153 The effects of warming on soil C stocks were variable, with positive, negative and neutral
154 impacts observed across sites (Figure 1). However, the direction and magnitude of these
155 warming-induced changes were predictable (Figure 2), being contingent upon the size of

156 standing soil C stocks and the extent and duration of warming. The interaction between
157 ‘control C stocks’ and ‘degree-years’ (the standardised metric to represent the
158 multiplicative product of the extent ($^{\circ}\text{C}$) and duration (years) of warming) was a strong
159 explanatory variable when predicting warmed C stocks (additive model AIC=383 vs.
160 multiplicative model AIC=381; see SI and Equation 1). Specifically, the impacts of
161 warming were negligible in areas with small initial C stocks, but losses occurred beyond a
162 threshold of 20 – 40 kg C m⁻³ and were considerable in soils with ≥ 60 kg C m⁻³ (Figure
163 1). No other environmental characteristics (mean annual temperature, precipitation, soil
164 texture or pH) significantly ($P > 0.1$) influenced the responses of soil C stocks to
165 warming in our statistical models (additive environmental with degree-year model
166 AIC=388; see SI).

167

168 The dominant role of standing C stocks in governing the magnitude of warming-induced
169 soil C losses is in line with both empirical and theoretical expectations^{2,15,16}. The thawing
170 of permafrost soils, where limited C decomposition has led to the accumulation of large
171 C stocks, will undoubtedly contribute to this phenomenon^{17,18}. However, our analysis also
172 revealed considerable soil C losses in several non-permafrost regions, suggesting that
173 additional mechanisms may contribute to the vulnerability of large soil C stocks.
174 Presumably, the vulnerability of soils containing large C stocks stems from the high
175 temperature-sensitivity of C decomposition and biogeochemical restrictions on the
176 processes driving soil C inputs. In ecosystems with low initial soil C stocks, minor losses
177 that result from accelerated decomposition under warming may be offset by concurrent
178 increases in plant growth and soil C stabilization^{12,19}. In contrast, in areas with larger
179 standing soil C stocks, accelerated decomposition outpaces potential C accumulation
180 from enhanced plant growth, driving considerable C losses into the atmosphere.

181

182 By combining our measured soil C responses with spatially-explicit estimates of standing
183 C stocks¹⁷ and soil surface temperature change²⁰ (using Equation 2), we reveal the global
184 patterns in the vulnerability of soil C stocks (Figure 3). Given that high-latitude regions
185 have the largest standing soil C stocks¹⁷ and the fastest expected rates of warming^{15,20},
186 our results suggest that the overwhelming majority of warming-induced soil C losses are

187 likely to occur in Arctic and sub-Arctic regions (Figure 3). These high-latitude C losses
188 drastically outweigh any minor changes expected in mid- and lower latitude regions,
189 providing additional support for the idea of Arctic amplification of climate change
190 feedbacks¹⁵ (Figure 3). These warming-induced soil C losses need to be considered in
191 light of future changes in moisture stress and vegetation growth, which are also likely to
192 respond disproportionately to climate change in high-latitude areas¹⁵. Notably, the spatial
193 distribution of soil C changes from our extrapolation contradicts projections from the
194 CMIP5 archive of Earth system models²¹, which show increases in soil C at high
195 latitudes, presumably due to the increases in plant productivity²². The warming-induced
196 losses of soil C that we observe have the potential to offset these vegetation responses,
197 emphasizing the importance of representing soil C vulnerability in the process-based
198 models used in climate change projections.

199

200 We extrapolated this relationship over the next 35 years to indicate how global soil C
201 stocks might respond by 2050. The simple extrapolation of our empirical relationship
202 suggests that 1 degree of warming over 35 years would drive the loss of 203 (± 161) Pg C
203 from the upper soil horizon (Figure 3). However, this approach implicitly assumes that
204 soil communities never acclimatize to changes in temperature, so are likely to drastically
205 over-estimate total soil C losses. Indeed, as with mechanistic models²³, our assumptions
206 about the rate of soil C acclimatization will strongly influence the magnitude of our
207 predicted C losses (see Figure 3B). For example, a range of recent analyses suggest that
208 soil communities can acclimatize to warming within a year²⁴⁻²⁶. If we assume annual
209 acclimatization to warming in our extrapolation, then approximately 30 (± 30) Pg C
210 would be lost from the surface soil for 1 degree ($^{\circ}\text{C}$) of warming. Given that global
211 average soil surface temperatures are projected to increase by ~ 2 $^{\circ}\text{C}$ over the next 35
212 years under a business-as-usual emissions scenario¹⁶, this annual time step extrapolation
213 would suggest that warming could drive the net loss of ~ 55 (± 50) Pg C from the upper
214 soil horizon. If, as expected, this C entered the atmospheric pool, it would increase the
215 atmospheric burden of CO_2 by approximately 25 ppm over this period.

216

217 The global extrapolation of our empirical data is broadly intended to contextualize our
218 measured changes in soil C stocks. We stress that such statistical approaches cannot be
219 used to project soil C losses far into the future because, unlike process-based models,
220 they cannot capture the complex processes that govern long-term C dynamics. For
221 example, extending the observed relationship over several centuries would lead to a
222 global convergence of soil C stocks. Conversely, soil C stocks would increase
223 exponentially in response to environmental cooling. Our linear extrapolation inherits
224 weaknesses from simple single pool models, which can over-predict the magnitude of
225 responses in the long term^{2,27}. However, the value of such linear approximations lie in
226 their descriptive strength rather than their predictive capabilities: instead of using short-
227 term flux estimates to project long-term changes in C stocks, our approach allows the
228 scaling of measured C differences over time frames (i.e. decades) represented by the
229 experimental studies. Our results capture the realised temperature-sensitivity of current
230 soil C stocks and can serve as a guideline (or target) for multi-pool process-based models.
231 Specifically, these models can run forward simulations that attempt to reflect the
232 outcomes of the warming experiments that we present. Those models which accurately
233 capture the observed relationships between standing soil C stocks and losses under
234 gradual step increases in global temperature are likely to be the most successful at
235 projecting the land C-climate feedback into the future.

236

237 Our analysis reveals a number of outstanding challenges facing empiricists and modelers,
238 which currently limit the certainty of current land C-climate feedback predictions (see
239 Supplementary Table 1). These limitations fall into two distinct categories, as more data
240 are necessary to improve (i) our current global estimates of soil C temperature sensitivity,
241 and (ii) modelling efforts to project these soil C responses into the future. First, along
242 with the limited spatial and temporal scale of current warming experiments, perhaps the
243 most critical limitation to our present analysis is the paucity of information about the
244 responses of soil C stocks at depth (below 10 cm). Although the size of C stocks decrease
245 down the soil profile²⁸, any additional C losses from these deeper soil horizons will
246 undoubtedly enhance the effects we present. Second, incorporating global soil C
247 information into modelling frameworks requires a mechanistic understanding of how

248 warming affects each of the individual components of the ecosystem C cycle. Now that
249 we are beginning to generate a global picture of the temperature-sensitivity of soil C
250 losses (respiration)⁸ and total C stocks, our limited understanding of how warming
251 influences global soil C inputs remains a major outstanding source of uncertainty for
252 modelling efforts^{1,22}. These efforts also require more information about the interacting
253 effects of other global change factors that may simultaneously influence soil C dynamics.
254 This non-exclusive set of practical challenges calls for concerted, coordinated investment
255 in multi-factor climate change experiments for an extended period of time to generate the
256 data necessary to improve confidence in future climate projections.

257

258 In conclusion, our global compilation of experimental data allows us to see past the
259 conflicting results from single-site studies and capture larger patterns in the sensitivity of
260 soil C to warming. The warming-induced changes in soil C stocks reflect the net result of
261 changes in C fluxes into and from the soil, which can augment modelling efforts to
262 project Earth system dynamics into the future. Ultimately, our analysis provides
263 empirical support for the long-held concern that rising temperatures stimulate the loss of
264 soil C into the atmosphere, driving a positive land C-climate feedback that could
265 accelerate planetary warming over the 21st century. Reductions in greenhouse gas
266 emissions are essential if we are to avoid the most damaging impacts of the land C-
267 climate feedback over the rest of this century.

268

269 REFERENCES

270

- 271 1. Todd-Brown, K. E. O. *et al.* Changes in soil organic carbon storage predicted by
272 Earth system models during the 21st century. *Biogeosciences* **11**, 2341–2356
273 (2014).
- 274 2. Jones, C. *et al.* Twenty-First-Century Compatible CO₂ Emissions and Airborne
275 Fraction Simulated by CMIP5 Earth System Models under Four Representative
276 Concentration Pathways. *J. Clim.* **26**, 4398–4413 (2013).
- 277 3. Arora, V. K. *et al.* Carbon–Concentration and Carbon–Climate Feedbacks in
278 CMIP5 Earth System Models. *J. Clim.* **26**, 5289–5314 (2013).

- 279 4. Ballantyne, A. P. *et al.* Audit of the global carbon budget: estimate errors and their
280 impact on uptake uncertainty. *Biogeosciences* **12**, 2565–2584 (2015).
- 281 5. Riahi, K. *et al.* RCP 8.5-A scenario of comparatively high greenhouse gas
282 emissions. *Clim. Change* **109**, 33–57 (2011).
- 283 6. Jobbágy, E. G. & Jackson, R. B. the Vertical Distribution of Soil Organic Carbon
284 and Its. *Ecol. Appl.* **10**, 423–436 (2000).
- 285 7. Bellamy, P. H., Loveland, P. J., Bradley, R. I., Lark, R. M. & Kirk, G. J. D.
286 Carbon losses from all soils across England and Wales 1978-2003. *Nature* **437**,
287 245–8 (2005).
- 288 8. Mahecha, M. D. *et al.* Global convergence in the temperature sensitivity of
289 respiration at ecosystem level. *Science* **329**, 838–40 (2010).
- 290 9. Davidson, E.A., Janssens, I. A. Temperature sensitivity of soil carbon
291 decomposition and feedbacks to climate change. *Nature* **440**, 165–73 (2006).
- 292 10. Crowther, T. W. *et al.* Biotic interactions mediate soil microbial feedbacks to
293 climate change. *Proc. Natl. Acad. Sci.* **112**, 7033–7038 (2015).
- 294 11. Lu, M. *et al.* Responses of ecosystem carbon cycle to experimental warming: a
295 meta-analysis. *Ecology* **94**, 726–738 (2013).
- 296 12. Day, T. a., Ruhland, C. T. & Xiong, F. S. Warming increases aboveground plant
297 biomass and C stocks in vascular-plant-dominated Antarctic tundra. *Glob. Chang.*
298 *Biol.* **14**, 1827–1843 (2008).
- 299 13. Sistla, S. a *et al.* Long-term warming restructures Arctic tundra without changing
300 net soil carbon storage. *Nature* **497**, 615–8 (2013).
- 301 14. Bradford, M. A., Wieder, W. R., Bonan, G. B., Fierer, N. Raymond, P. A. &
302 Crowther, T. W. Managing uncertainty in soil carbon feedbacks to climate change.
303 *Nat. Clim. Chang.* (2016). doi:10.1038/NCLIMATE3071
- 304 15. Serreze, M. C. & Barry, R. G. Processes and impacts of Arctic amplification: A
305 research synthesis. *Glob. Planet. Change* **77**, 85–96 (2011).
- 306 16. Koven, C. D. *et al.* A simplified, data-constrained approach to estimate the
307 permafrost carbon–climate feedback. *Philos. Trans. R. Soc. A Math. Phys. Eng.*
308 *Sci.* **373**, 20140423 (2015).
- 309 17. Hengl, T. *et al.* SoilGrids1km--global soil information based on automated

- 310 mapping. *PLoS One* **9**, e105992 (2014).
- 311 18. Schuur, E. A. *et al.* Climate change and the permafrost carbon feedback. *Nature*
312 **520**, 171–179 (2015).
- 313 19. Macias-Fauria, M., Forbes, B. C., Zetterberg, P. & Kumpula, T. Eurasian Arctic
314 greening reveals teleconnections and the potential for structurally novel
315 ecosystems. *Nat. Clim. Chang.* **2**, 613–618 (2012).
- 316 20. Meehl, G. a. *et al.* Climate change projections in CESM1(CAM5) compared to
317 CCSM4. *J. Clim.* **26**, 6287–6308 (2013).
- 318 21. Ciais, P. *et al.* in *Cli- mate Chang. 2013 Phys. Sci. Basis. Contrib. Work. Gr. I to*
319 *Fifth Assess. Rep. Intergov. Panel Clim. Chang.* (Stocker, T. F. *et al.*) (Cambridge
320 University Press, Cambridge, United Kingdom and New York, NY, USA., 2013).
- 321 22. Koven, C. D. *et al.* Controls on terrestrial carbon feedbacks by productivity versus
322 turnover in the CMIP5 Earth System Models. *Biogeosciences* **12**, 5211–5228
323 (2015).
- 324 23. Wieder, W. R., Bonan, G. B. & Allison, S. D. Global soil carbon projections are
325 improved by modelling microbial processes. *Nat. Clim. Chang.* **3**, 909–912 (2013).
- 326 24. Crowther, T. W. & Bradford, M. A. Thermal acclimation in widespread
327 heterotrophic soil microbes. *Ecol. Lett.* **16**, 469–77 (2013).
- 328 25. Bradford, M. A. Thermal adaptation of decomposer communities in warming soils.
329 *Front. Microbiol.* (2013).
- 330 26. Luo, Y., Wan, S.Q., Hui, D.F. & Wallace, L. L. Acclimatization of soil respiration
331 to warming in a tall grass prairie. *Nature* **413**, 622–625 (2001).
- 332 27. Georgiou, K., Koven, C. D., Riley, W. J. & Torn, M. S. Toward improved model
333 structures for analyzing priming: potential pitfalls of using bulk turnover time.
334 *Glob. Chang. Biol.* **21**, 4298–4302
- 335 28. Conant, R. T. *et al.* Temperature and soil organic matter decomposition rates -
336 synthesis of current knowledge and a way forward. *Glob. Chang. Biol.* **17**, 3392–
337 3404 (2011).
- 338
- 339
- 340

341

342 **AUTHOR CONTRIBUTIONS**

343 The study was conceived and designed by TWC and NS. Statistical analysis was
344 performed by KEOTB , MAB, and BLS. Spatial scaling and mapping was performed by
345 WRW and CWR. The manuscript was written by TWC with assistance from CWR,
346 MAB, WRW, KEOTB, SDA and PBR. All other authors reviewed and provided input on
347 the manuscript. Measurements of soil carbon, bulk density and geospatial data from
348 climate change experiments around the world were provided by JCC, MBM, SF, GZ,
349 AJB, BE, SR, AJH, HL, YL, AM, JP, ME, SDF, GK, CP, PHT, LLR, EP, SS, JML,
350 SDA, KKT, BE, LNM, IKS, KSL, YC, FAD, SM, SN, ATC, JMB, SB, JSC, FAD, JG,
351 BRJ, JM, LPM and PBR.

352

353 **ACKNOWLEDGEMENTS**

354 We would like to thank the Global Soil Biodiversity Initiative (GSBI) for support during
355 this project. This project was largely funded by grants to TWC from Marie Skłodowska
356 Curie, the British Ecological Society and the Yale Climate and Energy Institute. MAB
357 and WRW were supported by grants from the US National Science Foundation and
358 WRW from the US Department of Energy and KEOTB by the Linus Pauling
359 Distinguished Postdoctoral Fellowship program. The experiments that produced the data
360 were funded by grants too numerous to list here.

361

362

363 **FIGURE LEGENDS**

364

365 **Figure 1: The effect of warming on soil C losses depends on the initial standing soil**
366 **C stock.** The interaction between warming (degree-years) and standing C stocks is a
367 primary determinant of final warmed soil C stocks (estimated using a mixed effects
368 model; $n = 229$; see SI). Here, each point represents the difference (mean \pm SE) between
369 soil C stocks in warmed and ambient plots within an individual experiment. The size of
370 points represents the length of each individual study, and the colour indicates the amount

371 of warming. The shaded area represents the bootstrapped 95% confidence interval ($R^2 =$
372 0.49; see supplemental for details).

373

374 **Figure 2: Validation plots highlighting the predictive strength of the statistical**
375 **model.** Plate A: predicted vs. observed soil C stock values in warmed treatment plots
376 (estimated using statistical Equation 1: $R^2 = 0.95$ – high value is driven by the correlation
377 between C values in control and warmed plots). Black points represent mean values for
378 each study, and the coloured area represents the density of 1000 simulated points
379 randomly selected from within the normal distribution for each study. The 1:1 line is
380 included to highlight perfect correspondence between predicted and observed points and
381 distributions. Plate B: Bootstrapped estimates of model (Equation 2) slope values for
382 different sample sizes. Studies were removed at random, the slope coefficient was
383 calculated and this was repeated 1000 times. Each point represents a bootstrapped
384 estimate of slope for the model that included any given number of studies, and we include
385 the interquartile range and median slope estimates at each number. The average slope
386 value remains unchanged until >38 studies have been removed from the initial analysis
387 (with 49 studies), highlighting that the relationship we present is not disproportionately
388 influenced by the effects of warming in any specific study(s) or site(s).

389

390 **Figure 3: Spatial and temporal extrapolation of the temperature-vulnerability of soil**
391 **C stocks.** Plate A: Map of soil C vulnerability to warming. This map was generated by
392 extrapolating Equation 2 (i.e. the no-acclimation scenario) using spatially explicit
393 estimates of soil C stocks¹⁷, and soil surface temperature change²⁰, and reveals the spatial
394 variation in projected surface soil C stock changes (0-15 cm) expected under a 1°C rise in
395 global average soil surface temperature. Panel B: Total reductions in the global C pool
396 under a 1, and 2°C global average soil surface warming by 2050, as expected under a full
397 range of different soil acclimatization scenarios (x axis). Shaded areas indicate 95%
398 confidence intervals around the average C losses (dots) for each scenario. The rapid
399 acclimatization scenarios (e.g. 1 week – 1 year) result in lower total soil C losses than the
400 no acclimatization scenario, but all simulations reveal considerable global losses of soil C
401 under warming over the next 35 years. Note that our map predicts some C gains in desert

402 regions that currently contain almost no soil C. Removing these biochemically
403 questionable responses would marginally enhance the size of the global C losses reported
404 in Pannel B.

405

406

407 **METHODS**

408

409 **Data collection and standardisation**

410 Total percentage C and bulk density (BD) data (n=456) were collected from each of the
411 replicated warmed and ambient plots within 49 experimental warming studies located
412 across North America, Europe and Asia. In several of these sites, it was not possible to
413 access these data for deeper soil horizons. Therefore, we standardised collection
414 protocols and account for the considerable variability in soil horizon depths by focusing
415 on the top 10 cm of soil, which contains the majority of the biologically active C. Soil C
416 stocks were then calculated for each plot (percentage C * BD / 100), and expressed as the
417 total mass of C (kg m⁻³ soil) in each plot. Metadata for each study included the mean
418 annual difference in soil surface temperature between warmed and ambient plots and the
419 duration of experimental warming. These were multiplied together to generate the
420 standardised metric ‘degree-years’, (reflecting the extent and duration of warming) to
421 permit the comparison of warming effects across sites. Other collected data included a
422 site-specific geospatial reference (latitude and longitude), which was linked to spatially-
423 explicit estimates of soil characteristics (pH and texture using the SoilGrids database¹⁷)
424 and climate (using the Bioclim database) following Crowther *et al.*²⁹. These climate and
425 soil characteristics were then used to explore the dominant controls on soil C stock
426 sensitivity to warming across our global compilation of experimental studies.

427

428 Some of the climate change studies in this analysis contained multiple separate warming
429 experiments. Degree-years and soil C were calculated independently for each study
430 within a site, but all other environmental data were shared. In addition, some sites
431 included multi-factor climate change studies. For these studies, ambient and warmed

432 plots were only compared under equivalent experimental conditions so that all other
433 conditions remained consistent between treatments.

434

435 **Statistical analysis**

436 We fitted linear mixed models (LMMs) to evaluate the factors that correlate with the
437 measured soil C stocks following warming. Study site was included as a random factor
438 because clustering replicates by location could introduce spatial autocorrelation³⁰. The
439 LMMs were fit assuming a Gaussian error distribution in the “lme4” package for the R
440 statistical program³¹. We constructed LMMs that included all of the putative explanatory
441 variables to explain warmed soil C stocks including treatment variables (degrees warmed
442 and degrees warmed across years of study (degree-years)), and environmental
443 characteristics (Standing soil C stocks (control C stocks), Mean Annual Temperature
444 (MAT), Mean Annual Precipitation (MAP), pH (as H⁺ ion concentration) and soil texture
445 (with percentage clay as the representative variable)). Given the markedly different
446 ranges in magnitudes of the explanatory variables at a global scale, variables were
447 standardised using a z-transformation prior to use in final models³², though the response
448 variable (soil C stock) was not standardised. Further, given positive skew in the
449 distributions of degrees, degree-year and control soil C, these variables were also natural-
450 log transformed. Neither of these data transformations significantly altered the statistical
451 outputs, so were retained in final models. The only independent variables that were
452 strongly correlated (pairwise coefficients >0.4) were MAT and MAP, and MAT and
453 percentage clay.

454

455 Model selection was performed using maximum likelihood comparison of competing
456 models (see SI), using Akaike information criterion (AIC) and Bayesian information
457 criterion (BIC) approaches providing identical results. Only warming (degrees and
458 degree-years) and standing C stock (control soil C) were the most parsimonious final
459 models, (full model AIC=381 vs. final model AIC=372; Tables S6, S7) and the best-fit
460 model included an interaction between these two variables (additive model AIC=375 vs.
461 multiplicative model AIC=372; Table S7). All reported *P*-values are quasi-Bayesian,
462 rather than the classical frequentist *P*-values, but retain the same interpretation. We

463 considered coefficients with $P < 0.05$ significant and coefficients with $P < 0.10$ marginally
464 significant. Variance explained by the model was also estimated by calculating R^2 values
465 for the minimally-adequate LMM following Nakagawa and Schielzeth to retain the
466 random effects structure.

467

468 The final statistical model was:

$$469 \quad C_w = a \cdot C_c \cdot (DTDt) + b \cdot C_c + d \cdot (DTDt) + e \quad \text{Eqn 1}$$

470

471 where C_w is the carbon stock in the warmed treatment, C_c the carbon stock in the control
472 plots, $DTDt$ the degree-years calculated by multiplying the degrees warmed times the
473 length of the treatment, ε the random effects term controlling for study site (see SI), and
474 (a , b , d) represent fitted coefficients for the statistical model.

475

476 **Statistical model development**

477 To scale the changes in soil C stocks, we re-arranged our statistical equation in order to
478 describe the relationship between standing soil C stocks (control C stocks) and warming
479 (degree-years) over time:

480

$$481 \quad \frac{C_w - C_c}{DT \cdot Dt} = f \cdot C_c + g \quad \text{Eqn 2}$$

482

483 where C_w is the carbon stock in the warmed treatment, C_c the carbon stock in the control
484 plots, $DTDt$ the degree-years calculated by multiplying the degrees warmed times the
485 length of the treatment. This new model explained a considerable proportion ($R^2=0.606$;
486 SI Table 7) of the difference in soil C stocks between studies over treatment. This is
487 further highlighted in Figure 2.

488

489 We used sample-based bootstrapping (as opposed to the study-based bootstrapping in
490 Figure 2b) to evaluate the strength of this simple statistical relationship and to generate a
491 margin of error for global soil C stock projections. Equation 1 was extrapolated with
492 95%CI bounds by randomly selecting 200 samples from all studies, randomising the

493 control-warmed pairings, and repeating the regression 1000 times. This resulted in
494 normally distributed parameters (see SI Table 4) with the following 95%CI. The
495 intercept-slope pairs were then sampled to create the grey margin of error seen in Figure
496 1.

497

498 The inclusion of a linear effect of ‘time’ in our analysis implicitly assumes that soils
499 never acclimatize to warming. However, recent studies suggest that soils can acclimatize
500 to warming within an annual time-frame^{24–26}, so the assumption of no acclimatization is
501 likely to over-estimate total soil C losses. To explore the importance of this
502 acclimatization assumption in determining the magnitude of soil C losses in our
503 extrapolation, we repeated the analysis across a full range of acclimatization scenarios.
504 To simulate different acclimatization rates, we successively capped the study years (or
505 experiment duration) at 1 week, 1 month, 6 months, and 1, 5, 7, 8.75, 11.6, 17.5 years,
506 then re-ran the linear regression described above (Eqn 2) with the sample-based
507 bootstrapping. The resulting coefficients are in SI Table 4.

508

509 **Extrapolation**

510 To estimate changes in global soil C stocks under projected warming scenarios we
511 applied linear changes in soil temperature that result in 1 or 2°C mean warming by 2050
512 (35 years) that is spatially distributed in a manner consistent with surface soil temperature
513 projections from a single ensemble of the Community Earth System Model (CESM) that
514 was submitted to the CMIP5 archive under RCP8.5 run from 2005 to 2050. We estimated
515 initial soil C stocks in the upper soil horizon (0-15 cm) from the SoilGrids 50-
516 km² product¹⁷, that was regridded using bilinear interpolation to the same spatial scale of
517 soil surface temperature projections (roughly 1 degree).

518

519 The temporal extrapolations across the 35 years (until 2050) were applied separately for
520 each of the possible acclimatization scenarios described above. First, the single time step
521 approach used the coefficients listed above and illustrated in Figure 1 to generate a 95%
522 confidence interval for projected C losses. On average, roughly 17.5 degree-years and 35
523 degree-years were seen cumulatively across the globe for the 1 and 2°C warming

524 scenarios, respectively. The exact warming seen by any individual grid was determined
525 by their relative temperature shifts predicted by the CESM run described above. Each
526 subsequent acclimatization scenario was then extrapolated using a given time step for a
527 forward integration where the change in soil C over that time was based on the soil C
528 stock at the beginning and the degree-year change experienced by that site over the
529 duration of at respective time step. For example, the 1-year acclimation scenario used the
530 coefficients from the analysis where or experimental duration was capped at 1 year (see
531 SI, Table 4), and was extrapolated to 2050 using the sum of 35 annual time steps. The
532 predicted soil C losses for a global average warming of 1 and 2 C by 35 years, based on
533 each of the full range of acclimatization scenarios, is presented in Figure 3B. This reveals
534 how our assumption about acclimatization time influences the magnitude of our final
535 expected C losses.

536

537 The R code for the full analysis can be found in the Supplementary Material.

538

539 **References**

- 540 29. Crowther, T. W. *et al.* Mapping tree density at a global scale. *Nature* **525**, 201–205
541 (2015).
- 542 30. Bolker, B. M. *et al.* Generalized linear mixed models: a practical guide for ecology
543 and evolution. *Trends Ecol. Evol.* **24**, 127–135 (2009).
- 544 31. Bates, D., Machler, M., Bolker, B. M. & Walker, S. C. Fitting Linear Mixed-
545 Effects Models using lme4. *J. Stat. Softw.* **67**, 1–48 (2014).
- 546 32. Gelman, A. Scaling regression inputs by dividing by two standard deviations. *Stat.*
547 *Med.* **27**, 2865–2873 (2008).

548

549

550

551 **Extended data table 1:** List of current limitations in the availability of global data that
552 restrict confidence in our current understanding of the land C-climate feedback. Each of
553 these limitations represents a practical challenge that can be addressed by empiricists to
554 improve the accuracy of benchmarking estimates or to parameterize process-based

555 models that project Earth system dynamics into the future.

556

557 **Extended Data Figure 1:** Map of study locations. The size of points represents the
558 number of separate warming experiments at that location and colour indicates the biome,
559 as delineated by The Nature Conservancy (<http://www.nature.org>).

560

561 **Extended Data Figure 2:** Extended extrapolation of our linear model that illustrates
562 some of the limitations of this statistical scaling approach. Figures show soil C
563 projections for initial stocks under (A) 1 degree warming per decade, which converge on
564 the same soil C stocks; or (B) 2 degree cooling per decade, which show exponential
565 increases in soil C stocks. Although both of these responses are unrealistic, we note the
566 time scales (and amount of warming) needed to observe such dynamics are well outside
567 the range of observed manipulations or climate change projections. This highlights that
568 our extrapolation cannot represent a substitute for process-based models, which capture
569 long-term C dynamics. However, under more realistic warming (< 5 degrees C) our
570 extrapolation makes plausible projections over decadal time scale that represent the
571 current temperature sensitivity of soil C stocks.

572

573

574